ELSEVIER

Journal of Chromatography A, 686 (1994) 129–142

JOURNAL OF CHROMATOGRAPHY A

Separation and characterization of tetracycline antibiotics by capillary electrophoresis

Marina F.M. Tavares, Victoria L. McGuffin*

Department of Chemistry, Michigan State University, East Lansing, MI 48824, USA

First received 5 October 1993; revised manuscript received 28 June 1994

Abstract

The electrophoretic behavior of the antibiotics tetracycline, chlortetracycline, demeclocycline, oxytetracycline, doxycycline, methacycline and minocycline has been characterized by capillary electrophoresis in phosphate buffer solutions in the pH range 4–11. A complete set of acid–base equilibrium constants and electrophoretic mobilities was determined and, subsequently, was used in a computer-assisted optimization program to assess the separation of the tetracyclines. Under the predicted optimum conditions (pH 7.5, 18.2 m*M* ionic strength, 4.3 m*M* buffer concentration, and constant current of 20 μA), the separation was performed satisfactorily and all tetracyclines were readily identified. Moreover, the common impurities in tetracycline resulting from dehydration and epimerization reactions were discriminated under the same conditions. The determination of tetracycline, doxycycline and minocycline was performed in commercially available pharmaceutical formulations. During the dissolution of the contents of hard-filled capsules, a minimum recovery of 95% of the active ingredient was obtained. A calibration curve of peak height versus concentration gave a slope of $6.15 \cdot 10^{-4}$ cm M^{-1}, intercept of $-1.18 \cdot 10^{-5}$ cm, and coefficient of determination equal to 0.9989. The analysis using UV-absorbance detection at 260 nm provided a detection limit of $1 \cdot 10^{-5}$ *M* at a signal-to-noise ratio of approximately 3, with a linear range of two orders of magnitude.

1. Introduction

Tetracyclines are a group of clinically important natural products and semi-synthetic derivatives, characterized by a broad-spectrum activity against pathogenic microorganisms [1,2]. In addition to their extensive therapeutical use, these drugs have found application in the preservation of harvested fruits and vegetables, extermination of insect pests, and as an animal feed supplement [3–5].

All members of the group possess closely related chemical structures, derived from a common hydronaphthacene nucleus containing four fused rings [1,5], as shown schematically in Fig. 1. The presence of multiple functional groups with acid–base properties confers an amphoteric character to the tetracyclines, most of which exhibit an isoelectric point between 4 and 6. The same structural features contribute to their high solubility in polar organic solvents and water, which is enhanced at low pH. These compounds undergo complex formation and precipitation reactions with a variety of metallic cations, among which the complexes with calcium, mag-

* Corresponding author.

0021-9673/94/$07.00
SSDI 0021-9673(94)00668-7

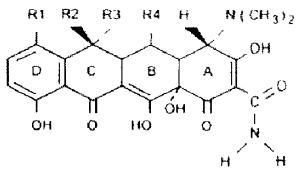

NAME	SYMBOL	R1	R2	R3	R4
TETRACYCLINE	TC	H	OH	CH_3	H
CHLORTETRACYCLINE	CTC	Cl	OH	CH_3	H
DEMECLOCYCLINE	DMCC	Cl	OH	H	H
OXYTETRACYCLINE	OTC	H	OH	CH_3	OH
DOXYCYCLINE	DOC	H	H	CH_3	OH
METHACYCLINE	MTC	H	$=CH_2$		OH
MINOCYCLINE	MNC	$N(CH_3)_2$	H	H	H

Fig. 1. Chemical structures of common tetracycline antibiotics.

nesium, and aluminum have been particularly well characterized [5].

Commercially available tetracycline and tetracycline derivatives may contain significant amounts of degradation products [6–8]. These contaminants are often isomers with only minor structural differences from the original precursor. The most important contaminants in tetracycline are the products of epimerization, dehydration and combined epimerization–dehydration reactions, as shown schematically in Fig. 2. Epianhydrotetracycline has been implicated in several toxic manifestations, such as renal dysfunction, caused by ingestion of degraded tetracycline products [1].

The analytical methodology applied to tetracyclines has supported microbiological production, synthetic and pharmacological studies and clinical applications. Several techniques have been employed [2,5,9], including microbiological assays [5], spectrophotometry [10–12], phosphorimetry [13], chemiluminescence [14], as well as chromatographic and flow injection methods [15]. Many of these methods do not provide a

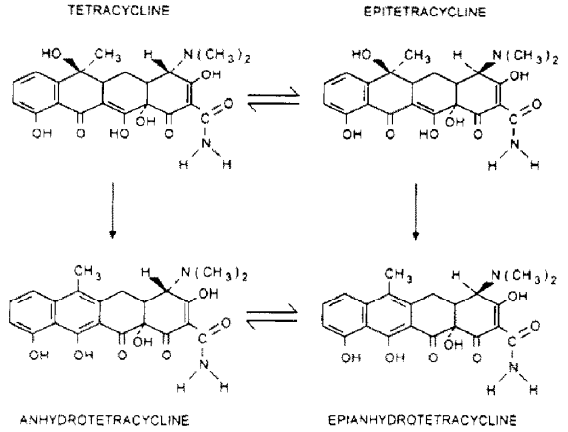

Fig. 2. Decomposition of tetracycline by epimerization and dehydration pathways.

precise and accurate means to determine the tetracycline content in the presence of known degradation products. In particular, the microbiological methods lack specificity, since the total drug activity is estimated without correlation to the chemical structure. Also, metabolites and degradation products with no antimicrobial activity cannot be determined by these methods. Among the chromatographic techniques, thin-layer, paper and column chromatography followed by UV spectrometric assay have been used extensively [16–22]. However, these methods have proven to be laborious, often require extensive sample pretreatment, and generally exhibit poor sensitivity and precision. Gas chromatographic methods, although rapid and specific, require derivatization of the polar functional groups under carefully controlled conditions. Consequently, their application is limited to antibiotics that are thermally stable after derivatization. Liquid chromatography, especially the reversed-phase and ion-exchange modes, has become the method of choice for tetracyclines in recent years [6–8,23–30]. Some of these procedures, however, use mobile phases of relatively low pH at which the tetracyclines are known to epimerize. Other methods employ mobile phases containing high salt concentration which, in combination with the low pH, can be deleterious to the column stability. Moreover, because of the structural similarities of the tetra-

cyclines and their potential contaminants, complete resolution is not usually achieved.

The physicochemical properties of tetracyclines, particularly their ionic nature, multiple ionization sites, and water solubility, make them suitable for electrophoretic analysis. Capillary electrophoresis (CE) has gained increased acceptance for the analysis of pharmaceuticals [9,31–34], as a result of relevant features such as high efficiency, high speed, full automation and compatibility with a variety of detection schemes. Based on the preliminary studies of antibiotics by Yeo et al. [34], we have explored the use of CE as a promising alternative to the available analytical methodologies for tetracyclines. A computer-assisted optimization program developed in previous work [35] was used to assess the separation of seven naturally occurring and synthetically produced tetracyclines, as well as their decomposition products. Based on this program, an optimized analytical method was developed and applied to the quantitation of tetracyclines in commercially available pharmaceutical drugs.

2. Experimental

2.1. Capillary electrophoresis system

The system consisted of a regulated high-voltage d.c. power supply (Model EH50R0.19XM6; Glassman High Voltage, Whitehouse Station, NJ, USA), operated under constant-current conditions. The power supply was connected via platinum rod electrodes to two small reservoirs containing the solution under investigation. Fused-silica capillary tubing (Polymicro Technologies, Phoenix, AZ, USA), with dimensions of 111.9 cm total length × 75 μm I.D. × 375 μm O.D., was immersed at each end in the solution reservoirs. The capillary surface was conditioned prior to use by rinsing with 1 *M* sodium hydroxide for 10 min, followed by rinsing with the solution under investigation, preferably overnight but at least for a 2-h period. During operation, the capillary was maintained at 25.0°C by means of a thermostatically controlled water bath (Model RTE 9B; Neslab Instruments, Portsmouth, NH, USA). Injection was performed hydrodynamically by maintaining a 2-cm difference in height between the liquid levels at the inlet and outlet reservoirs during a 1-min period. Detection was performed by means of an on-column UV-absorbance spectrophotometer (Model UVIDEC 100-V; Jasco, Tokyo, Japan), at a fixed wavelength of 260 nm. A detection window of 0.5 cm length was created by removing the polyimide coating from the capillary at a distance of 43.4 cm. The electroosmotic flow velocity was determined by the resistance-monitoring method [36].

2.2. Reagents

The phosphate buffer solutions were prepared from reagent-grade chemicals and deionized distilled water. In order to control both the buffer concentration and ionic strength, the solutions were formulated to contain sodium chloride in addition to the sodium salts of phosphoric acid. For any given pH, the total concentration of sodium was maintained constant and the ratio of sodium from each source, sodium chloride and buffer salts, was equal to unity. For determination of the acid–base equilibrium constants and electrophoretic mobilities, the buffer was varied from pH 4 to 11 with a total sodium concentration of 10 m*M*. For the separation of tetracycline standards and samples, the solutions were buffered at pH 7.5 with a total sodium concentration of 15 m*M*.

The antibiotics tetracycline (TC), chlortetracycline (CTC), demeclocycline (DMCC), oxytetracycline (OTC), doxycycline (DOC), methacycline (MTC) and minocycline (MNC) were obtained as reagent-grade standards (Sigma, St. Louis, MO, USA). Stock aqueous solutions of individual tetracycline standards as well as mixtures containing different combinations of the standards were prepared at a nominal concentration of 5 m*M* in pH 7.5 phosphate buffer solution. For the calibration curve, a 1 m*M* standard solution of tetracycline was diluted consecutively to 0.5, 0.1, 0.05 and 0.01 m*M* with the same buffer solution and was analyzed imme-

diately to prevent losses by adsorption on the glassware [37].

Pharmaceutical formulations of tetracycline (250 mg), doxycycline (50 mg) and minocycline (100 mg) were obtained as hard-filled capsules from Warner-Chilcott Labs. (Warner-Lambert, Morris Plains, NJ, USA). An appropriate mass of the drug was dissolved in pH 7.5 phosphate buffer to make a solution of 25 m*M* nominal concentration. The undissolved filler and binder materials were removed by centrifugation. An aliquot of the supernatant solution was then diluted to 5 m*M* concentration with pH 7.5 phosphate buffer solution and analyzed immediately.

In order to study the decomposition of tetracycline, a 25 m*M* solution was prepared by complete dissolution of an appropriate weight of the standard in hydrochloric acid at pH 2. This sample was heated at 70°C for 1 h, cooled in an ice bath, and then diluted to 5 m*M* concentration with pH 7.5 phosphate buffer solution. The sample was analyzed by reversed-phase liquid chromatography according to the method of Mack and Ashworth [7] in order to confirm the formation of the epi-, anhydro- and epianhydro-decomposition products of tetracycline.

2.3. Data processing

All data processing and numerical calculations were performed on a 80-386 microprocessor-based computer in a spreadsheet format (Microsoft Excel, version 4.0; Microsoft, Redmond, WA, USA). The optimization program developed in previous work [35] was written in the Forth-based programming language Asyst (version 2.1; Keithley Asyst, Rochester, NY, USA) to be executed on a 80-286 microprocessor-based computer.

3. Results and discussion

3.1. Characterization of the electrophoretic behavior of tetracyclines

In order to characterize the electrophoretic behavior of tetracyclines, knowledge of the acid–base equilibrium constants and electrophoretic mobilities of the individual species is required. The equilibrium constants (K_a) of very few tetracyclines have been reported in the literature [5]. After an initial misassignment [38] the attribution of pK_a values to specific functional groups in the molecule was reevaluated [39] and is now generally accepted. The most acidic group of tetracycline, with a typical pK_a value of approximately 3.3, is the hydroxyl group of the tricarbonyl system in ring A (Fig. 1). The second equilibrium constant, with a pK_a value of approximately 7.6, corresponds to the dicarbonyl system between rings B and C. The third constant, with a pK_a value of approximately 9.7, is assigned to the dimethylamine functionality in ring A. The highest equilibrium constant, with a pK_a of 10.7, was recently attributed to the phenolic group in ring D [39].

The electrophoretic determination of these constants is based on experimental measurements of effective mobility as a function of pH [35]. In CE, the effective mobility (μ_{eff}) of a solute (i) comprised of several species (j) in dynamic acid–base equilibrium, is related to the migration time of the substance (t_i) from the injector to the detector position (L_{det}) according to:

$$\mu_{eff,i} = \sum (\alpha_j \mu_j) = \frac{L_{tot} L_{det}}{V t_i} - \mu_{osm} \quad (1)$$

where L_{tot} is the total capillary length, V is the voltage, μ_{osm} is the electroosmotic mobility, μ_j is the electrophoretic mobility and α_j is the distribution function of species j. The distribution functions are related to the pH and to the acid–base equilibrium constants or pK_a values of the solutes under consideration [40]. Experimental values of the effective mobility, determined over a broad pH range, can be analyzed by a numerical regression procedure where the equilibrium constants and electrophoretic mobilities serve as adjustable parameters [35]. The best values for these parameters are then determined by the least-squares method. Table 1 presents the constants determined by the above procedure for seven members of the tetracycline group. All constants in Table 1 have been corrected to the

Table 1
Acid–base equilibrium constants and electrophoretic mobilities of tetracyclines at 25°C, corrected to the conditions of zero ionic strength

Solute	Equilibrium constant[a]					Electrophoretic mobility[a] ($\times 10^5$ cm^2 V^{-1} s^{-1})					
	$pK_{(+2,+1)}$	$pK_{(+1,0)}$	$pK_{(0,-1)}$	$pK_{(-1,-2)}$	$pK_{(-2,-3)}$	$\mu_{(+2)}$	$\mu_{(+1)}$	$\mu_{(0)}$	$\mu_{(-1)}$	$\mu_{(-2)}$	$\mu_{(-3)}$
TC	–	3.46	7.39	9.59	12.1	–	15.4	1.30	−15.2	−33.6	−64.7
CTC	–	3.60	7.52	9.88	10.4	–	19.5	−1.75	−19.1	−30.5	−43.8
DMCC	–	3.64	6.81	9.43	12.1	–	14.4	−0.04	−13.3	−36.8	−44.6
OTC	–	3.57	7.49	9.44	10.5	–	16.4	−0.60	−15.8	−34.7	−42.3
DOC	–	3.56	7.48	9.36	12.1	–	13.3	0.41	−12.5	−35.9	−57.7
MTC	–	3.56	7.29	9.46	12.0	–	14.3	0.02	−14.2	−34.4	−66.1
MNC	4.22[b]	4.22[b]	6.86	9.32	11.9	32.5	–	3.62	−7.75	−31.5	−53.7

[a] Subscripts denote charge of the species.
[b] Average pK_a corresponding to protonation of the amine groups in rings A and D (Fig. 1).

condition of zero ionic strength [41], and are in good agreement with values previously reported in the literature [39].

A graph of the effective mobility versus pH is a valuable tool for the preliminary assessment of a separation, because it can indicate regions of pH where the solute mobilities differ and the separation is likely to be achieved. The effective mobility curves displayed in Fig. 3A–C correspond to selected mixtures of tetracyclines containing four, five, and seven components, respectively. It is evident that the electrophoretic behavior of the tetracyclines is quite similar throughout the entire pH range and the separation appears to be very difficult. Consequently, a systematic procedure to determine the optimum separation conditions is highly desirable.

3.2. Optimization of the electrophoretic separation of tetracyclines

The separation of the tetracyclines was approached by means of a computer-assisted optimization routine developed in previous work [35]. In this approach, the quality of the separation is assessed by means of a response function developed originally for chromatographic separations [42], designated the chromatographic resolution statistic (CRS):

$$\mathrm{CRS} = \left\{ \sum_{i=1}^{n-1} \left[\frac{(R_{i,i-1} - R_{\mathrm{opt}})^2}{(R_{i,i+1} - R_{\mathrm{min}})^2 R_{i,i+1}} \right] + \sum_{i=1}^{n-1} \frac{R_{i,i+1}^2}{(n-1)R_{\mathrm{avg}}^2} \right\} \cdot \frac{t_f}{n} \quad (2)$$

where $R_{i,i-1}$ is the resolution between pairs of adjacent solute zones, R_{avg} is the average resolution of all solute pairs, R_{opt} is the optimum desired resolution, R_{min} is the minimum acceptable resolution, t_f is the migration time of the last solute, and n is the number of solutes in the sample. The chromatographic resolution statistic considers the resolution of all solutes in the sample, rather than solely the least-resolved pair, and incorporates three important aspects of the separation. The first term in Eq. 2, named the resolution term, evaluates the resolution between all adjacent solute zones in comparison to the defined values for optimum and minimum resolution. The resolution term decreases as $R_{i,i+1}$ approaches R_{opt} and reaches the minimum value of zero when $R_{i,i+1}$ is exactly equal to R_{opt}. Any further increase in resolution offers no additional improvement in the quality of the separation, hence the resolution term is maintained at a constant value close to zero. The resolution term increases rapidly as $R_{i,i+1}$ approaches R_{min} and becomes undefined when $R_{i,i+1}$ is exactly equal to R_{min}. The second term

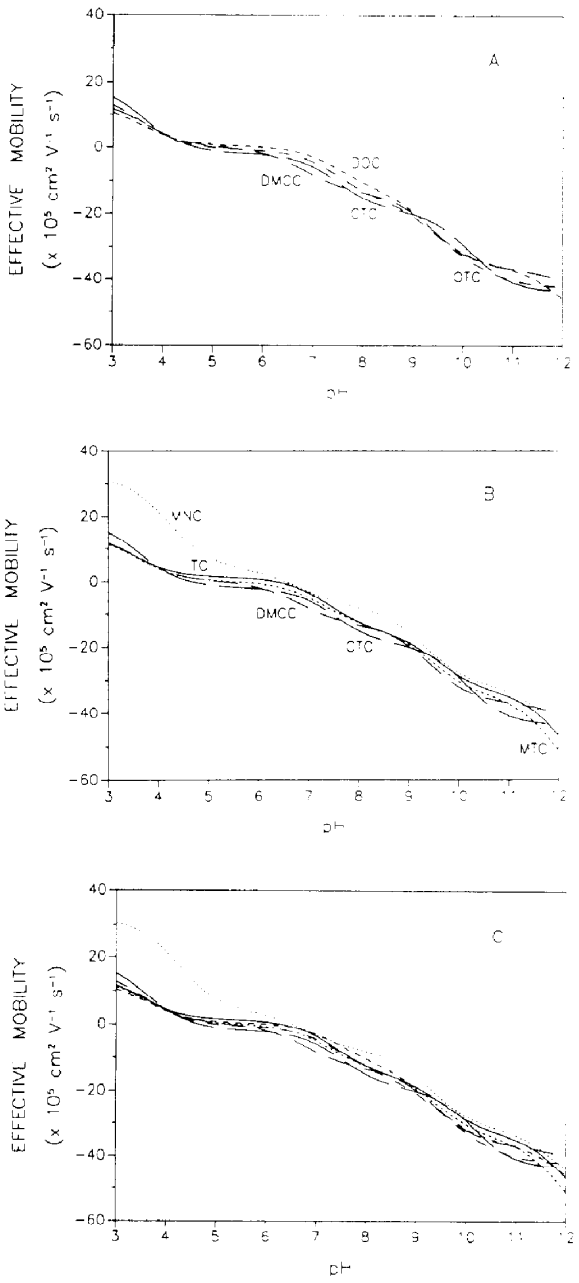

Fig. 3. Effective mobility curves as a function of pH for selected four- (A), five- (B) and seven- (C) component mixtures of tetracyclines at 25°C, corrected to the conditions of zero ionic strength.

of Eq. 2, named the distribution term, considers the relative spacing of the solute zones. The distribution term approaches a minimum value of unity when the resolution of each solute pair is equal to the average resolution, which is the case when all zones are uniformly spaced. The final multiplier term in Eq. 2 takes into consideration the analysis time and the complexity of the sample.

The resolution between adjacent solute zones is defined as the difference between their mean migration time (t) divided by their average temporal base width (w):

$$R_{i,i+1} = \frac{2(t_{i+1} - t_i)}{w_i + w_{i+1}} \tag{3}$$

The migration time of each zone to the detector position is determined by the net rate of zone migration (v_i), which is a vectorial summation of the electrophoretic (v_{ep}) and electroosmotic (v_{osm}) velocities:

$$t_i = \frac{L_{det}}{v_i} = \frac{L_{det}}{v_{ep} + v_{osm}} = \frac{L_{det} L_{tot}}{(\mu_{ep} + \mu_{osm})V} \tag{4}$$

According to Eq. 4, the prediction of migration time requires knowledge of the electrophoretic and electroosmotic mobilities. Hence, the computer program is structured on theoretical models for these migration processes that are applicable under a variety of operational conditions. The electrophoretic migration subroutine is based on classical equilibrium calculations [35] and requires as input the acid–base equilibrium constants and electrophoretic mobilities of the tetracyclines (Table 1). The electroosmotic migration may be determined from experimental measurements or, if not available, from a theoretical model. In this model [36], a mathematical function that relates the zeta potential to the pH and sodium concentration of the buffer solution is utilized to calculate the electroosmotic mobility.

The base width of a normally distributed zone is proportional to the standard deviation of the temporal distribution (τ):

$$w_i = 4\tau \tag{5}$$

where τ is expressed in time units, and is related

to the standard deviation of the spatial distribution (σ) by means of the zone velocity:

$$\tau = \frac{\sigma}{v_i} \quad (6)$$

The variance of the spatial distribution (σ^2) arises from several dispersive phenomena that occur during the migration of the solute zone. If these processes are independent, then the variances are statistically additive [43]:

$$\sigma^2 = \sum \sigma_n^2 \quad (7)$$

where σ_n^2 represents the individual contributions to the total variance. Among the dispersive mechanisms, the contributions to the zone variance resulting from longitudinal diffusion as well as finite injection and detection volumes are considered in the optimization program.

An overall expression for resolution in Eq. 3 can be derived by combining appropriately Eqs. 4–7. The resolution of each solute pair is then used to determine the overall quality of the separation by means of the CRS function in Eq. 2. In order to implement these calculations, input values for parameters related to the buffer composition (pH, ionic strength and concentration), capillary dimensions (diameter and length), and instrumental parameters (applied voltage or current) must be specified. By methodically varying these parameters and evaluating the overall quality of the separation by means of the CRS function, the computer program can be used to predict the experimental conditions required for optimal separation of the solutes.

The optimization of the tetracycline separation was simulated using instrumental parameters and capillary dimensions that are representative of the experimental system (see above). In the search for the optimum conditions, the current was varied from 5.00 to 22.50 μA with increments of 0.25 μA, the pH from 4.0 to 11.0 with 0.1 increments, the ionic strength from 5.00 to 22.50 mM with 0.25 mM increments, and the buffer concentration from 0.50 to 11.00 mM with 0.15 mM increments. The surface maps and corresponding contour plots presented in Figs. 4 and 5 allow for visual inspection of the CRS response function within the defined range of parameters. Although there are several local minima of the CRS function, the most promising region occurs between pH 7 and 8. Within this region, the CRS function decreases rapidly as the current approaches 20 μA (Figs. 4A and 5A). The function behaves similarly as the buffer concentration approaches 4 mM (Figs. 4B and 5B). In contrast, the ionic strength surface map is composed of several very sharp minima in the region between 15 and 20 mM, which indicates that this variable must be controlled carefully.

The computer program predicts the correct elution order for all tetracyclines, and provides a reasonable estimate of migration time and peak width, as demonstrated in Table 2. The agreement between predicted and experimental values for migration time and peak width is typically 1.7 and 23%, respectively.

3.3. *Analytical determination of tetracyclines*

The experimental separation of the seven tetracyclines was performed in the vicinity of the optimal conditions, as shown in Fig. 6C. Because of similarities in the equilibrium constants and mobilities of the tetracyclines, complete separation is not possible under the predicted optimum conditions. However, qualitative analysis may be performed since all tetracyclines may be identified unequivocally in the mixture. Quantitative analysis is possible for selected mixtures containing four and five tetracyclines (Fig. 6A and B, respectively), as suggested by visual inspection of the effective mobility curves (Fig. 3A and B, respectively). This analysis represents an improvement over the available methodology for tetracyclines, since there is a substantial gain in efficiency (ca. $3 \cdot 10^4$ theoretical plates) and reduction in analysis time (< 6 min). Reversed-phase liquid chromatographic methods, which are among the most commonly employed methods for tetracyclines, provide efficiencies on the order of $3 \cdot 10^3$ plates and analysis times as long as 30 min for typical mixtures [2].

A common concern during the manufacture and storage of tetracycline antibiotics is the control of impurities. Tetracyclines can degrade

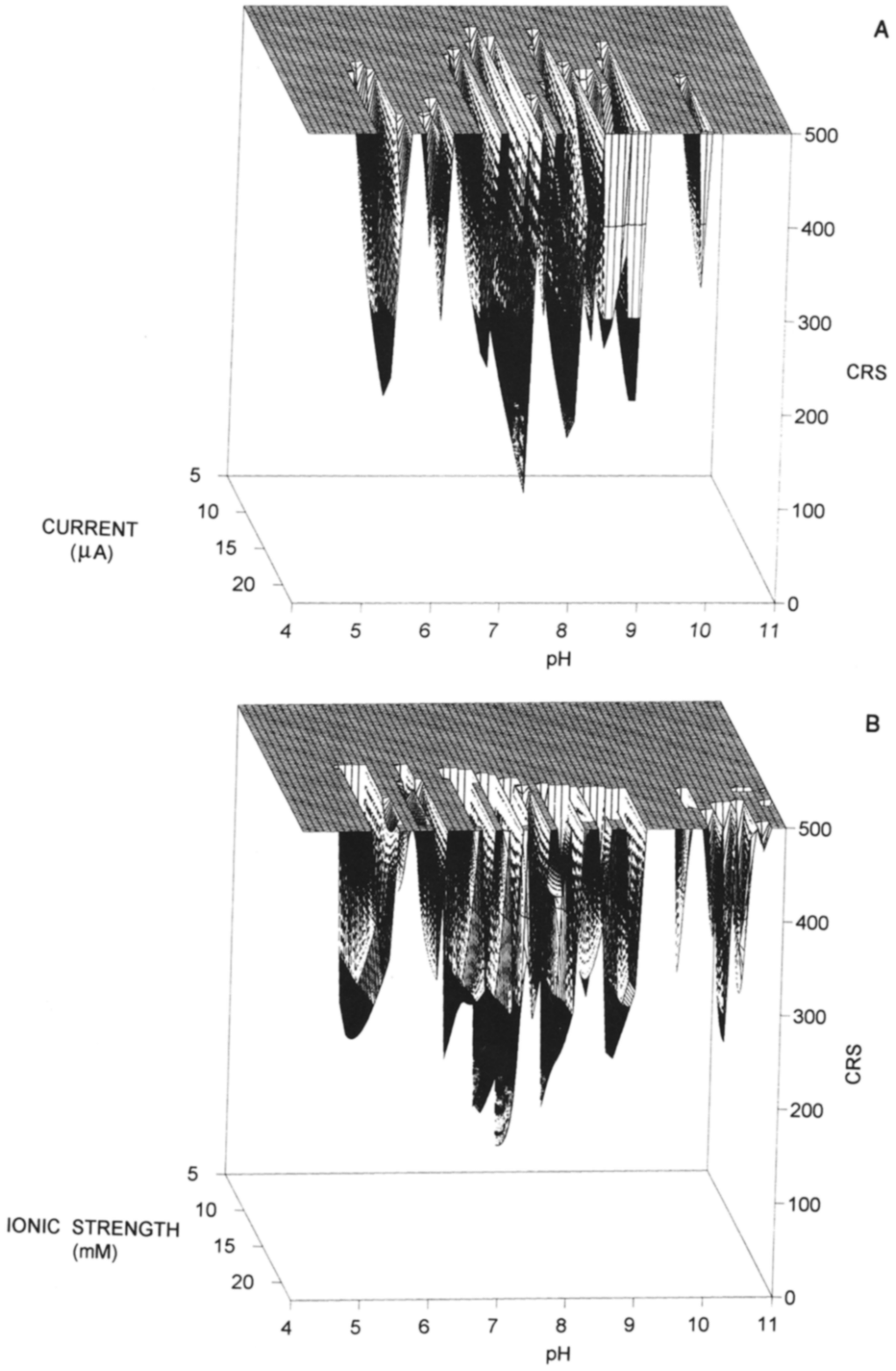
A
500
400
300
CRS
200
100
0
5
10
15
20
CURRENT
(μA)
4
5
6
7
8
9
10
11
pH
B
500
400
300
CRS
200
100
0
5
10
15
20
IONIC STRENGTH
(mM)
4
5
6
7
8
9
10
11
pH

Fig. 4.

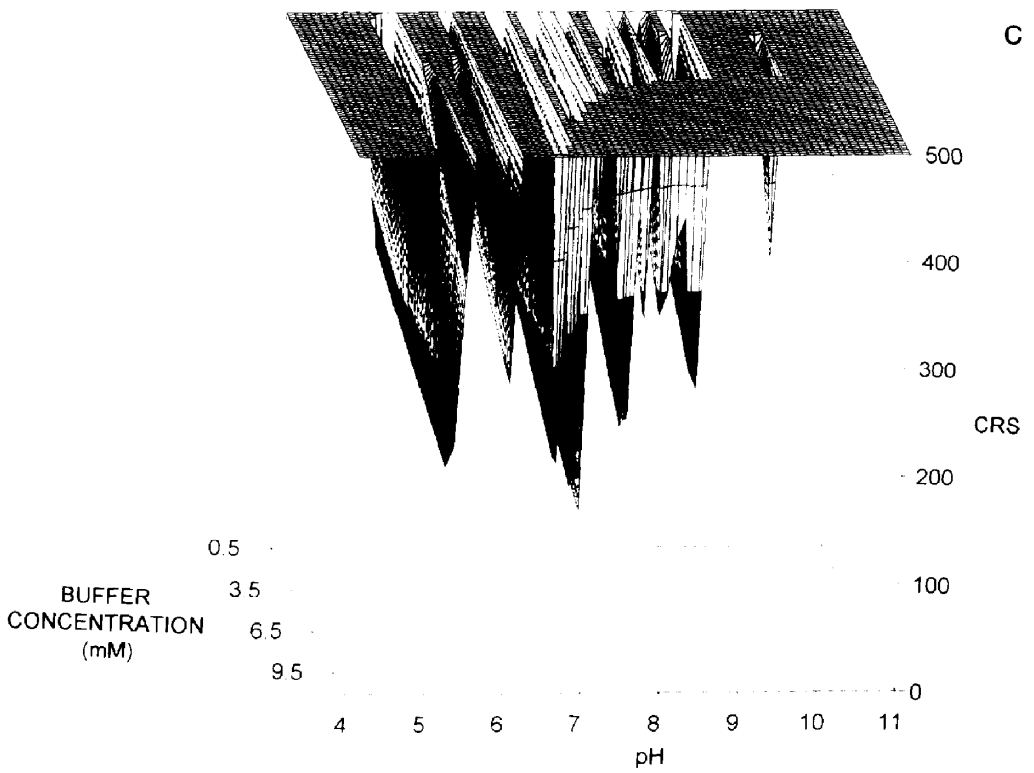

Fig. 4. Surface maps representing the separation of tetracyclines by CE. (A) CRS as a function of pH and applied current with constant ionic strength of 18 m*M* and buffer concentration of 4.5 m*M*. (B) CRS as a function of pH and ionic strength with constant buffer concentration of 4.5 m*M* and current of 20 μA. (C) CRS as a function of pH and buffer concentration with constant ionic strength of 18 m*M* and current of 20 μA.

through at least four different mechanisms, epimerization, dehydration, hydrolysis and oxidation, where the former two are the most important processes [5]. The epimerization of the dimethylamine group in ring A of tetracycline produces the inactive and non-toxic epitetracycline (Fig. 2). The dehydration followed by aromatization of ring C produces anhydrotetracycline, which is also inactive and nontoxic. Both epimerization of anhydrotetracycline and dehydration of epitetracycline lead to the formation of the inactive, but rather toxic epianhydrotetracycline. The kinetics of the epimerization and dehydration reactions have been extensively studied [5,44,45], indicating that these processes can be accelerated at very low pH and under high-temperature conditions. In Fig. 7A and B, the electropherogram of a tetracycline standard is displayed together with a sample that was previously decomposed by heating under acidic conditions. Although primary standards were not available, the decomposition products may be tentatively identified based on the observed changes in electrophoretic mobility. The dehydration reaction decreases the molecular mass and produces a more planar structure, both of which result in an increase in the electrophoretic mobility of anhydrotetracycline relative to that of tetracycline. The epimerization reaction changes the structural features only slightly, resulting in a small decrease in the mobility of the epimers relative to those of tetracycline and anhydrotetracycline. Because the decomposition products are well resolved from the principal component, this method can be used to identify and quantitate tetracycline and its impurities in commercially available pharmaceutical formulations, as demonstrated in Fig. 7C.

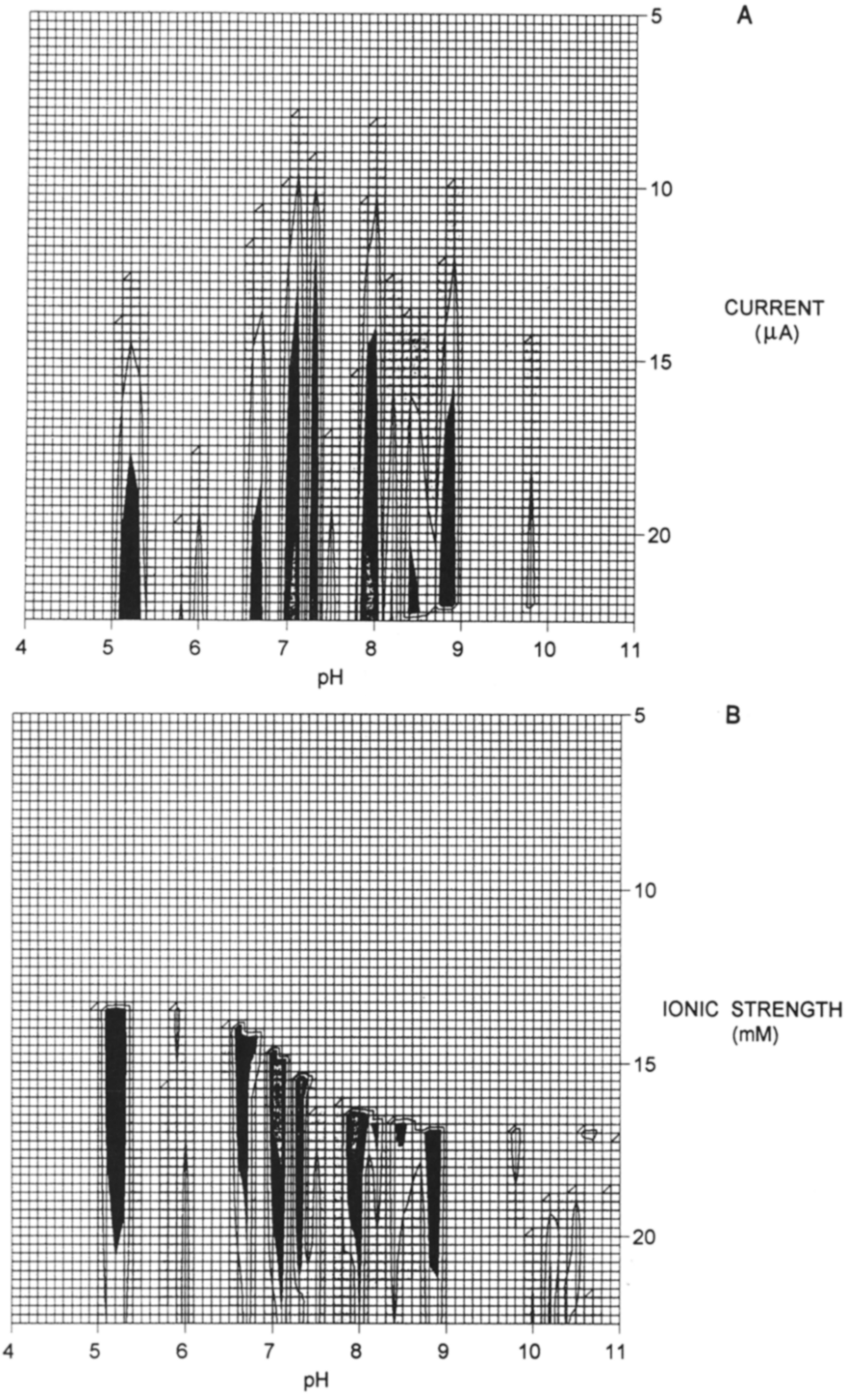
A
5
10
15
20
CURRENT
(μA)
4
5
6
7
8
9
10
11
pH
B
5
10
15
20
IONIC STRENGTH
(mM)
4
5
6
7
8
9
10
11
pH

Fig. 5.

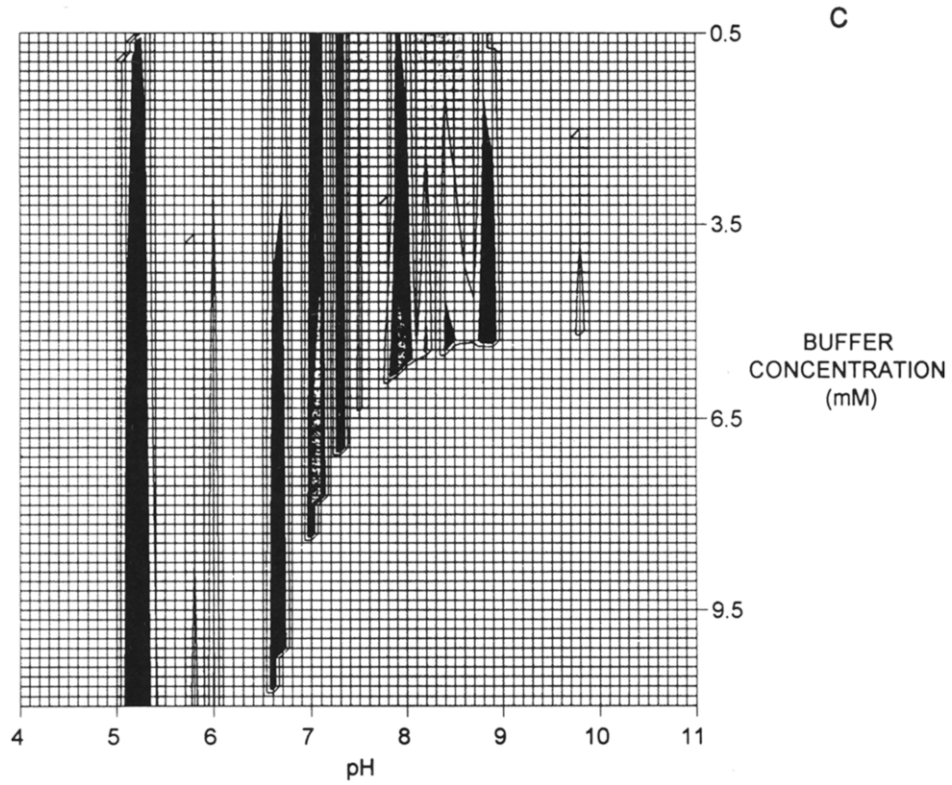

Fig. 5. Contour maps representing the separation of tetracyclines by CE. (A) CRS as a function of pH and applied current with constant ionic strength of 18 m*M* and buffer concentration of 4.5 m*M*. (B) CRS as a function of pH and ionic strength with constant buffer concentration of 4.5 m*M* and current of 20 μA. (C) CRS as a function of pH and buffer concentration with constant ionic strength of 18 m*M* and current of 20 μA.

Table 2
Comparison of experimentally (Exp) determined migration time and base width of tetracyclines with computer-simulated (Calc) values in the vicinity of the optimum conditions (pH 7.5, ionic strength 18.2 m*M*, buffer concentration 4.3 m*M* and constant-current conditions of 20 μA)

Solute	Migration time (min)			Width (min)		
	Exp	Calc[a]	Error (%)[b]	Exp	Calc[c]	Error (%)[b]
MNC	5.05	5.03	0.4	0.085	0.098	−15
DOC	5.16	5.14	0.4	0.068	0.100	−47
TC	5.25	5.24	0.2	0.081	0.102	−26
OTC	5.41	5.30	2.0	0.081	0.104	−29
MTC	5.48	5.32	2.9	0.085	0.104	−22
CTC	5.59	5.46	2.3	0.115	0.107	+7.0
DMCC	5.71	5.49	3.9	0.123	0.108	+12

[a] Calculated from Eq. 1 with an experimentally determined electroosmotic mobility of $6.40 \cdot 10^{-4}$ cm^2 V^{-1} s^{-1}.
[b] Error (%) = 100(Exp − Calc)/Exp.
[c] Calculated from Eqs. 5–7 with theoretical contributions to spatial variance of $5.34 \cdot 10^{-3}$ to $5.80 \cdot 10^{-3}$ cm^2 for diffusion, $1.78 \cdot 10^{-2}$ cm^2 for injection and $2.08 \cdot 10^{-2}$ cm^2 for detection [35].

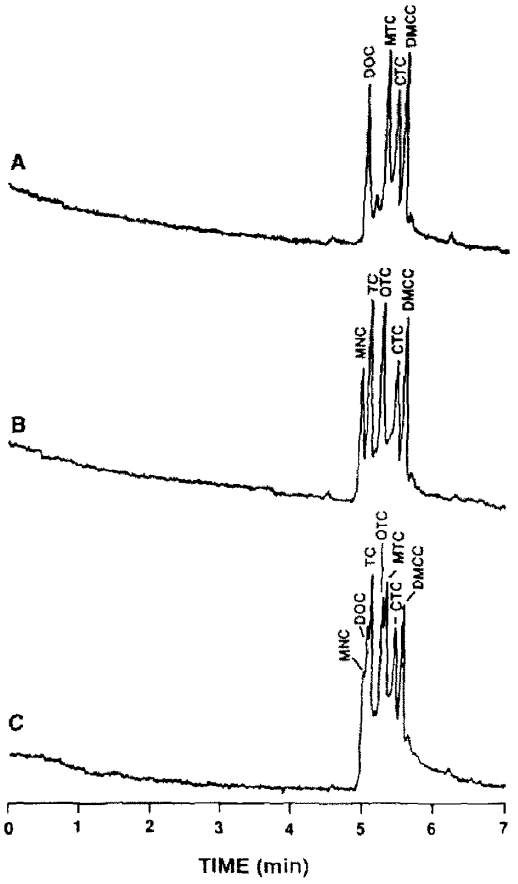

Fig. 6. Separation of selected four- (A), five- (B) and seven- (C) component mixtures of tetracyclines by CE in the vicinity of the optimum conditions identified from Figs. 4 and 5. Experimental conditions: pH 7.5 phosphate buffer, buffer concentration 4.3 mM, total sodium concentration 15 mM, ionic strength 18.2 mM and applied current of 20 μA.

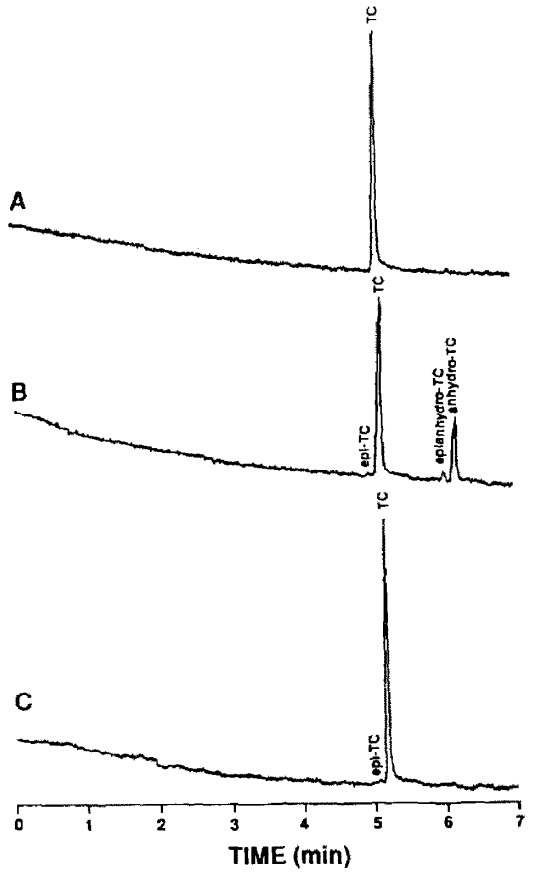

Fig. 7. Electrophoretic separation of tetracycline and its decomposition products under the optimized experimental conditions given in Fig. 6. (A) Tetracycline standard. (B) Tetracycline standard previously treated with pH 2 hydrochloric acid at 70°C for 1 h. (C) Tetracycline pharmaceutical formulation as hard-filled capsules.

In the analysis of tetracycline in hard-filled capsules, a minimum recovery of 95% of the active ingredient was obtained. A calibration curve of peak height versus concentration gave a slope of $6.15 \cdot 10^{-4}$ cm M^{-1}, intercept of $-1.18 \cdot 10^{-5}$ cm, and coefficient of determination equal to 0.9989. The detection limit was $1 \cdot 10^{-5}$ M at a signal-to-noise ratio of approximately 3 [46], with a linear range of two orders of magnitude. In addition to tetracycline, other commercially available pharmaceutical formulations were examined, such as doxycycline and minocycline, with comparable analytical figures of merit.

Among the tetracyclines characterized in this work, chlortetracycline presented the most unusual electrophoretic behavior, as illustrated in Fig. 8. The chlortetracycline standard exhibits a marked asymmetry in the direction of a contaminant, which possesses a migration time coincident with that of tetracycline. Chlortetracycline is known to decompose to form tetracycline under relatively mild conditions [47–49]. The results presented herein suggest that this decomposition may be enhanced by application of an electric field. Consequently, electrophoretic techniques may not be suitable to monitor

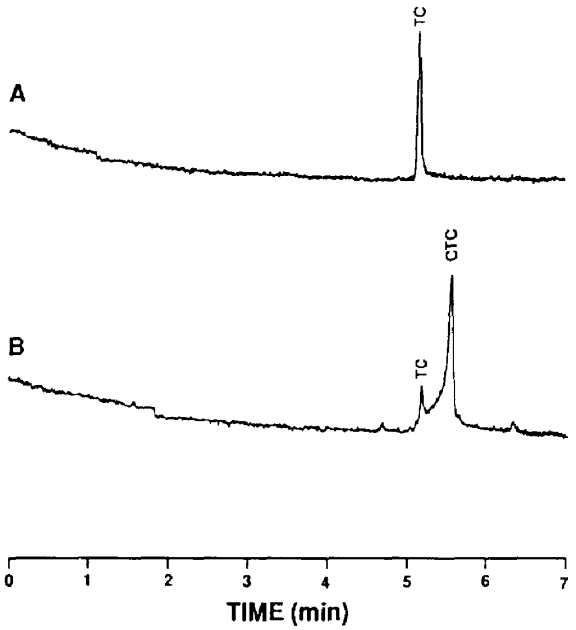

Fig. 8. Electrophoretic behavior of chlortetracycline under the optimized experimental conditions given in Fig. 6. (A) Tetracycline standard. (B) Chlortetracycline standard.

chlortetracycline in pharmaceutical formulations. It is noteworthy that the decomposition of chlortetracycline had a deleterious effect upon the separation shown in Fig. 6C. In the absence of this zone asymmetry, resolution is significantly improved and qualitative and quantitative analysis of the tetracyclines is more accurately achieved (Fig. 9).

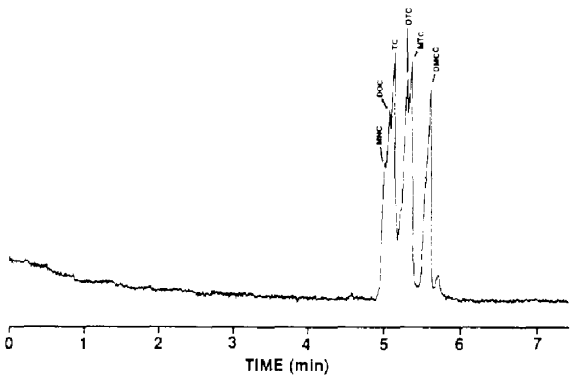

Fig. 9. Electrophoretic separation of tetracyclines in the absence of chlortetracycline under the optimized experimental conditions given in Fig. 6.

4. Conclusions

In this work, CE was characterized as a resourceful analytical method for tetracycline, its natural and synthetic analogues, as well as common impurities arising during manufacture or from decomposition during storage. The electrophoretic behavior of seven members of the group was thoroughly studied in the pH range 4–11, and a complete set of acid–base equilibrium constants and electrophoretic mobilities was derived. These constants were used as input to a computer program, which established the optimal conditions for the separation. The analysis of tetracyclines in pharmaceutical formulations was satisfactorily achieved under the predicted optimum conditions.

Acknowledgements

This research was supported by the US Department of Energy, Office of Basic Energy Sciences, Division of Chemical Sciences, under contract number DE-FG02-89ER14056. Additional support was provided by the Dow Chemical Co. and Eli Lilly Co. The authors acknowledge Dr. Gerald Larson (Michigan State University) for the pharmaceutical samples. M.F.M.T. gratefully acknowledges a fellowship from the Conselho Nacional de Desenvolvimento Científico e Tecnológico (CNPq) of Brazil.

References

[1] H.P. Lambert and F.W. O'Grady, *Antibiotic and Chemotherapy*, Churchill Livingstone, London, 6th ed., 1992.

[2] A. Aszalos, *Modern Analysis of Antibiotics, Drugs and the Pharmaceutical Sciences*, Vol. 27, Marcel Dekker, New York, 1986.

[3] A.P. De Leenheer and H.J.C.F. Nelis, *J. Pharm. Sci.*, 68 (1979) 999–1002.

[4] J.P. Sharma, E.G. Perkins and R.F. Bevill, *J. Chromatogr.*, 134 (1977) 441–450.

[5] L.A. Mitscher, *The Chemistry of the Tetracycline Antibiotics (Medicinal Research Series*, Vol. 9), Marcel Dekker, New York, 1978.

[6] J. Hermansson and M. Andersson, *J. Pharm. Sci.*, 71 (1982) 222–229.
[7] G.D. Mack and R.B. Ashworth, *J. Chromatogr. Sci.*, 16 (1978) 93–101.
[8] K. Tsuji and J.H. Robertson, *J. Pharm. Sci.*, 65 (1976) 400–404.
[9] R.K. Gilpin and L.A. Pachla, *Anal. Chem.*, 65 (1993) 117R–132R.
[10] H. Ping-Kay and F. Wai-Kwong, *Analyst*, 116 (1991) 751–752.
[11] K.M. Emara, H.F. Askal and G.A. Saleh, *Talanta*, 38 (1991) 1219–1221.
[12] U. Saha, A.K. Sen, T.K. Das and S.K. Bhowal, *Talanta*, 37 (1990) 1193–1196.
[13] J.X. Duggan, *J. Liq. Chromatogr.*, 14 (1991) 2499–2525.
[14] A.B. Syropoulos and A.C. Calokerinos, *Anal. Chim. Acta*, 255 (1991) 403–411.
[15] A.A. Alwarthan, S.A. Al-Tamrah and S.M. Sultan, *Analyst*, 116 (1991) 183–186.
[16] W. Naidong, S. Hua, E. Roets and J. Hoogmartens, *J. Planar Chromatogr.-Mod. TLC*, 5 (1992) 92–98.
[17] W. Naidong, C. Hauglustaine, E. Roets and J. Hoogmartens, *J. Planar Chromatogr.-Mod. TLC*, 4 (1991) 63–68.
[18] W. Naidong, S. Hua, K. Verresen, E. Roets and J. Hoogmartens, *J. Pharm. Biomed. Anal.*, 9 (1991) 717–723.
[19] K.J. Kovács-Hadady, *J. Planar Chromatogr.-Mod. TLC*, 4 (1991) 456–459.
[20] W. Naidong, S. Geelen, E. Roets and J. Hoogmartens, *J. Pharm. Biomed. Anal.*, 8 (1990) 891–898.
[21] W. Naidong, T. Cachet, E. Roets and J. Hoogmartens, *J. Planar Chromatogr.-Mod. TLC*, 2 (1989) 424–429.
[22] J.S. Kang and S.J. Ebel, *J. Planar Chromatogr.-Mod. TLC*, 2 (1989) 434–437.
[23] N.H. Khan, P. Wera, E. Roets and J. Hoogmartens, *J. Liq. Chromatogr.* 13 (1990) 1351–1374.
[24] W. Naidong, E. Roets and J. Hoogmartens, *J. Pharm. Biomed. Anal.*, 7 (1989) 1691–1703.
[25] A. Aszalos, C. Haneke, M.J. Hayden and J. Crawford, *Chromatographia*, 15 (1982) 367–373.
[26] J.H. Knox and J. Jurand, *J. Chromatogr.*, 186 (1979) 763–782.
[27] A.P. De Leenheer and H.J.C.F. Nelis, *J. Chromatogr.*, 140 (1977) 293–299.
[28] J.H. Knox and J. Jurand, *J. Chromatogr.*, 110 (1975) 103–115.
[29] E.R. White, M.A. Carrol, J.E. Zarembo and A.D. Bender, *J. Antibiot.*, 28 (1975) 205–214.
[30] A.G. Butterfield, D.W. Hughes, N.J. Pound and W.L. Wilson, *Antimicrob. Ag. Chemother.*, 4 (1973) 11–15.
[31] P.D. Grossman and J.C. Colburn (Editors), *Capillary Electrophoresis —Theory and Practice*, Academic Press, San Diego, CA, 1992.
[32] M.T. Ackermans, J.L. Beckers, F.M. Everaerts and I.G.J.A. Seelen, *J. Chromatogr.*, 590 (1992) 341–353.
[33] M. Lookabaugh, M. Biswas and I.S. Krull, *J. Chromatogr.*, 549 (1991) 357–366.
[34] S.K. Yeo, H.K. Lee and S.F.Y. Li, *J. Chromatogr.*, 585 (1991) 133.
[35] M.F.M. Tavares and V.L. McGuffin, *Anal. Chem.*, in press.
[36] M.F.M. Tavares and V.L. McGuffin, *Anal. Chem.*, in press.
[37] A.E. Ciarlone, B.W. Fry and D.M. Ziemer, *Microchem. J.*, 42 (1990) 250–255.
[38] L.I. Leeson, J.E. Krueger and R.A. Nash, *Tetrahedron Lett.*, 18 (1963) 1155–1160.
[39] N.E. Rigler, S.P. Bag, D.E. Leyden, J.L. Sudmeier and C.N. Reilley, *Anal. Chem.*, 37 (1965) 872–875.
[40] J.N. Butler, *Ionic Equilibrium —A Mathematical Approach*, Addison-Wesley, Reading, MA, 1964.
[41] R.A. Robinson and R.H. Stokes, *Electrolyte Solutions —The Measurement and Interpretation of Conductance, Chemical Potential and Diffusion in Solutions of Simple Electrolytes*, Butterworths, London, 1959.
[42] T.D. Schlabach and J.L. Excoffier, *J. Chromatogr.*, 439 (1988) 173–184.
[43] J.C. Giddings, *Unified Separation Science*, Wiley-Interscience, New York, 1991.
[44] K.D. Schlecht and C.W. Frank, *J. Pharm. Sci.*, 64 (1975) 352–354.
[45] B.A. Hoener, T.D. Sokoloski, L.A. Mitscher and L. Malspeis, *J. Pharm. Sci.*, 63 (1974) 1901–1904.
[46] P.A. St. John, W.J. McCarthy and J.D. Winefordner, *Anal. Chem.*, 39 (1967) 1495–1497.
[47] W. Naidong, E. Roets, R. Busson and J. Hoogmartens, *J. Pharm. Biomed. Anal.*, 8 (1990) 881–889.
[48] M. Sokolic, B. Filipovic and M. Pokorny, *J. Chromatogr.*, 509 (1990) 189–193.
[49] W. Naidong, E. Roets and J. Hoogmartens, *Chromatographia*, 30 (1990) 105–109.